Dyes and Pigments 163 (2019) 318–329

Contents lists available at ScienceDirect

Dyes and Pigments

journal homepage: www.elsevier.com/locate/dyepig

Molecular structure and spectral properties of indolenine based norsquaraines *versus* squaraines

Olga S. Kolosova[b], Svitlana V. Shishkina[b,c], Vered Marks[a], Gary Gellerman[a], Iryna V. Hovor[b], Anatoliy L. Tatarets[b], Ewald A. Terpetschnig[d], Leonid D. Patsenker[a,*]

[a] Department of Chemical Sciences, The Faculty of Natural Sciences, Ariel University, Ariel, 40700, Israel
[b] SSI "Institute for Single Crystals" of the National Academy of Sciences of Ukraine, 60 Nauky Ave., Kharkov, 61001, Ukraine
[c] V. N. Karazin Kharkiv National University, 4 Svobody Sq., Kharkiv, 61022, Ukraine
[d] SETA BioMedicals, 2014 Silver Court East, Urbana, IL, 61802, USA

ARTICLE INFO

Keywords:
Norsquaraine
Squaraine
Molecular structure
Simulations
BSA-Complexes
Spectral properties

ABSTRACT

Novel indolenine based norsquaraine dyes, wherein the oxygen of the squaric acid bridge was substituted with a barbituric or a dicyanomethylene group, were synthesized and their molecular structure, spectral and luminescent properties were compared to those of analogous squaraine dyes. The molecular structure was investigated using X-ray analysis, NMR spectroscopy and *ab initio* DFT B3LYP/6-311G (d, p) simulations. The calculated populations of possible conformers and the barriers of internal rotations were found to be in good agreement with the experimental data. Norsquaraines absorb and emitt light within the same long-wavelength spectral range as the corresponding squaraines but due to intramolecular *H*-bonds and increased conformational rigidity they were less sensitive to solvent polarity and the presence of protein (BSA).

1. Introduction

Squaraine dyes are a subclass of cyanines that contain a 3-oxocyclobut-1-enolate (squarate) moiety in the polymethine chain [1–3]. Due to their excellent spectral characteristics such as the long-wavelength absorption and emission, high molar absorptivity, high fluorescence quantum yields, and stability, squaraines are widely used as fluorescent probes and labels for biomedical assays [4–6], clinical diagnostics [7,8], pharmaceutical research [9,10], as sensitive dyes in electronics [11], sensitizers for photovoltaic cells [12] and sunlight energy converters [13]. The molecular structure of these dyes was investigated using various experimental [14–17] and theoretical methods [18]. The spectral properties of squaraines [19], their complexes [20,21] and conjugates [22,23] with proteins were also thoroughly studied. Squaraine dyes comprising *indolenine* based terminal end groups are of most interest in particular for biomedical applications due to their increased brightness and photostability [24]. Squaraines may be substituted with various ionic and other functional groups at the indolenine nitrogens, which facilitate their solubility in hydrophobic or hydrophilic media [25,26] and reaction with biomolecules [27].

Nevertheless, the molecular structure and spectral properties of indolenine based squaraines containing hydrogen atoms at the indolenine nitrogens, so-called *norsquaraines*, have not been sufficiently investigated [28,29]. The simplest norsquaraine **nor-SqO** was synthesized and its molecular structure was simulated by the semiempirical methods AM1 and PM3 [30]. The calculations carried out in this publication predicted coexistence of very polar *cis,syn*-conformer labeled as ISQ4 (C_{2v} symmetry) as the major component and non-polar centrosymmetric *trans,anti*-conformer ISQ6 (C_{2h} symmetry) as the minor component while the ^{1}H NMR data evidenced the opposite conformer population. The molecular geometry of **nor-SqO** investigated by X-ray analysis was affected by the interaction with two $CHCl_3$ molecules existed in the unit cell, which did not allow to conclude on the anticipated dominant conformer in solutions [31].

* Corresponding author.
E-mail addresses: kolosova@isc.kharkov.com (O.S. Kolosova), sveta@xray.isc.kharkov.com (S.V. Shishkina), veredma@ac.ariel.il (V. Marks), garyg@ariel.ac.il (G. Gellerman), govor@isc.kharkov.com (I.V. Hovor), tatarets@isc.kharkov.com (A.L. Tatarets), ewaldte@setabiomedicals.com (E.A. Terpetschnig), leonidpa@ariel.ac.il, leonid.patsenker@gmail.com (L.D. Patsenker).

https://doi.org/10.1016/j.dyepig.2018.12.007
Received 21 October 2018; Received in revised form 28 November 2018; Accepted 5 December 2018
Available online 10 December 2018
0143-7208/

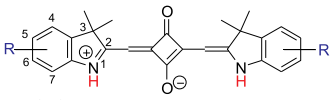

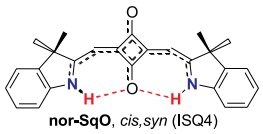

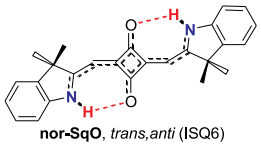

The PCM-PBE0/6-31 + G(d,p) calculations of **nor-SqO** [32] predicted that the conformer ISQ6 was 0.5 kcal/mol more stable than ISQ4. Other conformers had much higher energies and had no effect on these populations. It was demonstrated also that the absorption and emission spectra of **nor-SqO** could be described as a combination of the electronic spectra of these two forms.

A few substituted norsquaraines **1a–1f** were also synthesized but their molecular structures and fluorescence properties were not investigated [33]. Importantly, to the best of our knowledge, no other norsquaraine derivatives were reported until now.

This work investigates the molecular structures and spectral properties of **nor-SqO** and its novel, first synthesized derivatives, where the squaric oxygen is substituted with a barbituric (**nor-SqB**) and dicyanomethylene **(nor-SqCN**) group, and compares these properties with those of conventional, previously reported squaraines **SqO** and **SqCN** [34] and a newly synthesized squaraine **SqB**.

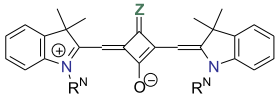

nor-SqO: Z = O, R^N = H
nor-SqB: Z = barbituric, R^N = H
nor-SqCN: Z = C(CN)$_2$, R^N = H
SqO: Z = O, R^N = Me
SqB: Z = barbituric, R^N = Me
SqCN: Z = C(CN)$_2$, R^N = Me

2. Materials and methods

2.1. General information

Iodomethane and 2,3,3-trimethylindolenine were purchased from *Acros*; 3,4-dihydroxy-3-cyclobutene-1,2-dione (squaric acid) was from *Aldrich*; Bovine Serum Albumin (BSA, essentially fatty acid free), Silica gel 60 for column chromatography and other materials were from *Merck* and used as received. Phosphate buffer (PB) pH 7.4 (67 mM) was prepared by dissolving $Na_2HPO_4{\cdot}2H_2O$ (9.596 g) and KH_2PO_4 (1.743 g) in 1 L distilled water.

Mass spectra were measured by a *BIFLEX III MALDI-TOF* mass spectrometer using 2,5-dihydroxybenzoic acid was taken as the matrix. FAB mass spectra were recorded on a *SELMI MI-1201E* instrument using 3-nitrobenzylalcohol (NBA) or glycerol as a matrix.

The ***C, H, N elemental analysis*** was performed by a *EuroVector Euro EA* 3000 EA-*IRMS* elemental analyzer.

^{1}H NMR and ^{13}C NMR spectra were measured on a *Varian Mercury-VX-200* (^{1}H 200 MHz) spectrometer in DMSO-d_6 using signal of remaining non-deuterated solvent as an internal standard (2.50 ppm for DMSO). Selected spectra (^{1}H 400 MHz and ^{13}C 100 MHz) were recorded in $CDCl_3$ using a 400 MHz *Bruker Avance^{III} HD*. BBI probe was equipped with Z-axis gradients coils. TMS was used as an internal standard (0.00 ppm). A full assignment was done using 2D experiments: COSY (^{1}H–^{1}H correlation), HMQC, HMBC (^{1}H–^{13}C short and long correlation, respectfully) and *J*-resolved. ^{1}H NOESY experiments employed 128 t_1 increments with a dwell time of 83.2 μs and a mixing time of 1.5 s. A recycle delay of 2.5 s was used in all NMR experiments.

X-Ray diffraction analysis. The dark-blue crystals with metallic luster of **nor-SqO** ($C_{26}H_{24}N_2O_2$) were obtained by recrystallization from 1-propanol with 0.1% diethylamine. Crystals are monoclinic. At 293 K a = 18.1805(8), b = 6.4028(3), c = 18.7430(8) Å, β = 107.185(5)°, V = 2084.4(2) Å^3, M_r = 396.28, Z = 4, space group $P2_1/n$, d_{calc} = 1.263 g/cm^3, μ(MoK$_\alpha$) = 0.080 mm^{-1}, $F(000)$ = 840. Intensities of 20723 reflections (4757 independent, R_{int} = 0.025) were measured on the *Xcalibur-3* diffractometer (graphite monochromated MoK$_\alpha$ radiation, CCD detector, ω-scanning, $2\Theta_{max}$ = 55°). The structure was solved by direct method using SHELXTL package [35]. Positions of the hydrogen atoms were located from electron density difference maps and refined by "riding" model with $U_{iso} = nU_{eq}$ (n = 1.5 for methyl hydrogens and n = 1.2 for other hydrogen atoms) of the carrier atom. The hydrogen atoms at the indolenine nitrogens were refined using isotropic approximation. Full-matrix least-squares refinement against F^2 in anisotropic approximation for non-hydrogen atoms using 4649 reflections was converged to wR_2 = 0.127 (R_1 = 0.044 for 2936 reflections with $F > 4\sigma(F)$, S = 0.972). The final atomic coordinates, and crystallographic data for **nor-SqO** molecule have been deposited to the Cambridge Crystallographic Data Center, 12 Union Road, CB2 1EZ, UK (fax: +44-1223-336033; e-mail: deposit@ccdc.cam.ac.uk) and are available on request quoting the deposition numbers CCDC 998817).

Absorption spectra were recorded for the dye concentrations c_{Dye} ~0.5 μM in phosphate buffer (PB) 7.4 and other solvent systems discussed below. All the absorption spectra were recorded in 1-cm quartz cells at 25 °C using a *PerkinElmer Lambda 35* UV/Vis spectrophotometer. Absorption maxima were determined with an accuracy of ± 0.5 nm and rounded off.

Molar absorptivity (ε). The investigated dye (7–10 mg) was dissolved in the solvent of interest (50 mL), the stock solution was diluted to the dye concentration c_{Dye} ~ 0.5 μM and the absorbance (A) in the absorption band maximum was measured in a 5-cm standard quartz cell. The molar absorptivity were calculated according to the Beer—Lambert law. The molar absorptivityý of each dye was independently measured three times and the average value was taken. The reproducibility for determining the molar absorptivity was within ± 2000 M^{-1}cm^{-1}.

Emission spectra and quantum yields were measured for dye concentrations c_{Dye} ~0.5 μM in PB pH 7.4 and other solvents listed below. The excitation wavelength was 620 nm. The fluorescence measurements were done in 1-cm standard quartz cells at 25 °C using a *Varian Cary Eclipse* spectrofluorometer. The emission spectra were corrected for wavelength-dependent instrument sensitivity. Emission maxima were determined with an accuracy of ± 1.0 nm.

Spectral characteristics of dyes in presence of BSA (dye—BSA complexes) were measured at c_{Dye} = 0.5 μM and BSA concentration c_{BSA} = 90 μM (6 g/L).

Quantum chemical ab initio simulations were carried out using Density Functional Theory (DFT) and B3LYP functional [36] with 6-311G(d,p) basis sets [37] within the Gaussian 09 program [38]. The vibrational frequencies were calculated and no imaginary frequencies were found for the equilibrium geometries. The NPA charges were calculated using the NBO pro6 program [39].

Populations of the conformers (c, %) was calculated for 25 °C according to the Boltzmann distribution.

2.2. Synthesis

General procedure. A mixture of quaternized or non-quaternized indolenine (2 mmol) and squaric acid or its dicyanomethylene or barbituric derivative was refluxed in 50 mL of a butanol—toluene mixture (1:1, v/v). The solvent was removed and the residue was dried in a vacuum desiccator over P_2O_5. The product was column purified (Silica gel 60, $CHCl_3$—MeOH, gradient).

2-(3,3-dimethyl-2,3-dihydro-1*H*-2-indolylidenmethyl)-4-(3,3-dimethyl-3*H*-2-indoliumylmethylene)-3-oxo-1-cyclobuten-1-olate

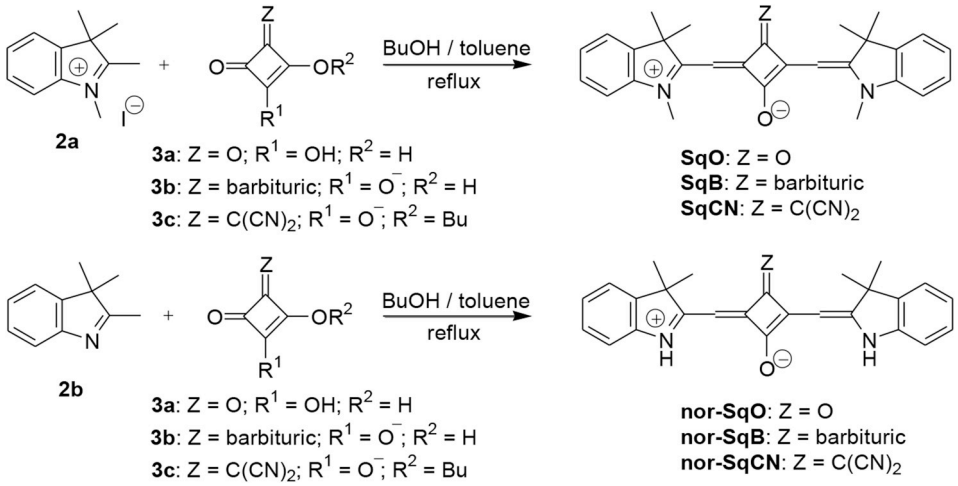

Scheme 1. Synthesis of squaraines and norsquaraines.

(**nor-SqO**): Yield 75%. Dark-blue solid. ^{1}H NMR (400 MHz, $CDCl_3$, ppm): Major conformer: δ 12.84 (2H, N*H*, broad s), 7.27 (2H, arom-*ortho*, d, J = 7.6 Hz), 7.25 (2H, arom-*meta*, m, second order), 7.13 (2H, arom-*ortho,*d, J = 7.8 Hz), 7.08 (2H, arom-*meta*. ddd, J = 7.6, 7.5, 0.8 Hz), 5.48 (2H, C*H*, s), 1.453 (12H, CH_3, s). Minor conformer: δ 12.54 (2H, N*H*, broad s), 7.27 (2H, arom-*ortho*, d, J = 7.6 Hz), 7.25 (2H, arom-*meta*, m, second order), 7.13 (2H, arom-*ortho,*d, J = 7.8 Hz), 7.08 (2H, arom-*meta*, ddd, J = 7.6, 7.5, 0.8 Hz), 5.52 (2H, C*H*, s), 1.450 (12H, CH_3, s). ^{13}C NMR (100 MHz, $CDCl_3$, ppm): Major conformer: δ 183.42 (*C*O), 175.77 (C*C*NH), 175.14 (CH*C*$(CO)_2$), 141.96 (arom, *C*), 139.02 (arom, *C*), 128.29 (arom, *C*H), 123.20 (arom, *C*H), 122.35 (arom, *C*H), 111.51 (arom, *C*H), 85.94 (*C*H), 48.70 (-*C*$(CH_3)_2$), 26.65 (CH_3). Minor conformer: 185.59 (*C*O), 180.31 (CO), 175.91(C*C*NH), 175.24 (CH*C*$(CO)_2$), 141.86 (arom, *C*), 139.02 (arom, *C*), 128.24 (arom, *C*H), 123.26 (arom, *C*H), 122.48 (arom, *C*H), 111.36 (arom,*C*), 86.17 (*C*H), 48.70 (-*C*$(CH_3)_2$), 26.65 (CH_3). MALDI-TOF MS, *m/z* calcd. for $[C_{26}H_{24}N_2O_2]^+$ 396.2, found: 397.1 $[M+H]^+$, 419.0 $[M+Na]^+$, 434.9 $[M+K]^+$. Anal. calcd. (%) for $C_{26}H_{24}N_2O_2$: C, 78.76; H, 6.10; N, 7.07. Found: C, 78.72; H, 6.12; N, 7.12.

2-(1,3,3-trimethyl-2,3-dihydro-1*H*-2-indolylidenmethyl)-4-(1,3,3-trimethyl-3*H*-2-indoliumylmethylene)-3-oxo-1-cyclobuten-1-olate (**SqO**): Yield 78%. Dark-blue solid. ^{1}H NMR (400 MHz, DMSO-d_6, ppm): δ 7.51 (2H, arom. H, d, J = 7.2 Hz), 7.37–7.32 (4H, arom. H, m), 7.18–7.15 (2H, arom. H, m), 5.76 (2H, C*H*, s), 3.57 (6H, NCH_3, s), 1.69 (12H, (CH_3)$_2$, s). ^{1}H NMR (400 MHz, $CDCl_3$, ppm): δ 7.33 (2H, arom. H, m), 7.16–7.13 (2H, arom. H, t, J = 7.2 Hz), 7.00 (2H, arom. H, d, J = 7.6 Hz), 5.91 (2H, C*H*, s), 3.56 (6H, NCH_3, s), 1.77 (12H, (CH_3)$_2$, s). ^{13}C NMR (100 MHz, $CDCl_3$, ppm): δ 182.53 (*C*O), 180.31 (C*C*NCH_3), 170.94 (CH*C*$(CO)_2$), 143.20 (arom, *C*), 127.95 (arom, *C*), 123.91 (arom, *C*H), 122.24 (arom, *C*H), 109.31 (arom, *C*H), 99.23(arom, *C*H), 86.88 (*C*H), 49.38 (-*C*$(CH_3)_2$), 30.73(CH_3), 27.22 (CH_3). FAB MS, *m/z* calcd. for $[C_{28}H_{28}N_2O_2]^+$ 424.22, found: 424.3 $[M^+]$, 425.3 $[MH^+]$. Anal. calcd. (%) for $C_{26}H_{24}N_2O_2$: C, 78.76; H, 6.10; N, 7.07. Found: C, 78.72; H, 6.12; N, 7.12.

2-(3,3-dimethyl-2,3-dihydro-1*H*-2-indolylidenmethyl)-4-(3,3-dimethyl-3*H*-2-indoliumylmethylene)-3-(2,4,6-trioxohexahydro-5-pyrymidinylidene)-1-cyclobuten-1-olate (**nor-SqB**): Yield 16%. Dark-green solid. ^{1}H NMR (400 MHz, DMSO- d_6, ppm): δ 12.19 (2H, N*H*, s) 10.27 (2H, N*H*-barb, s), 7.53 (2H, arom. H, d, J = 7.6 Hz), 7.39–7.33 (4H, arom. H, m), 7.18–7.15 (2H, arom. H, m), 6.63 (2H, C*H*, s), 1.44 (12H, (CH_3)$_2$, s). FAB MS, *m/z* calcd. for $[C_{30}H_{26}N_4O_4]^+$ 506.20, found: 507.1 $[M+H]^+$. Anal. calcd. (%) for $C_{30}H_{26}N_4O_4$: C, 71.13; H, 5.17; N, 11.06. Found: C, 71.12; H, 5.13; N, 11.10.

2-(1,3,3-trimethyl-2,3-dihydro-1*H*-2-indolylidenmethyl)-4-(1,3,3-trimethyl-3*H*-2-indoliumylmethylene)-3-(2,4,6-trioxohexahydro-5-pyrymidinylidene)-1-cyclobuten-1-olate (**SqB**): Yield 39%. Dark-green solid. H NMR (400 MHz, DMSO-d_6, ppm): δ 10.02 (2H, N*H*, s), 7.55 (2H, arom. H, d, J = 7.2 Hz), 7.42–7.36 (4H, arom. H, m), 7.24 (2H, arom. H, t, J = 6.8 Hz), 6.45 (2H, C*H*, s), 3.58 (6H, NCH_3, s), 1.66 (12H, (CH_3)$_2$, s). FAB MS, *m/z* calcd. for $[C_{32}H_{30}N_4O_4]^+$ 534.23, found: 535.2 $[M+H]^+$. Anal. calcd. (%) for $C_{32}H_{30}N_4O_4$: C, 71.89; H, 5.66; N, 10.48. Found: C, 71.85; H, 5.62; N, 10.50.

3-Dicyanomethylene-2-(3,3-dimethyl-2,3-dihydro-1*H*-2-indolylidenmethyl)-4-(3,3-dimethyl-3*H*-2-indoliumylmethylene)-1-cyclobuten-1-olate (**nor-SqCN**): Yield 35%. Dark-green solid. ^{1}H NMR (400 MHz, DMSO-d_6, ppm): δ 12.00 (2H, N*H*, s), 7.54 (2H, arom. H, d, J = 7.2 Hz), 7.39–7.33 (4H, arom. H, m), 7.19 (2H, arom. H, t, J = 6.8 Hz), 5.69 (2H, C*H*, s), 1.44 (12H, (CH_3)$_2$, s). ^{13}C NMR (100 MHz, $CDCl_3$, ppm): δ 178.58, 176.87, 163.00, 162.57, 141.34, 139.46, 128.56, 124.36, 122.81, 117.01, 111.95, 87.16, 49.68, 46.39, 26.45. FAB MS, *m/z* calcd. for $[C_{29}H_{24}N_4O]^+$ 444.20, found: 445.1 $[M+H]^+$. Anal. calcd. (%) for $C_{29}H_{24}N_4O$: C, 78.36; H, 5.44; N, 12.60. Found: C, 78.32; H, 5.49; N, 12.65.

3-Dicyanomethylene-2-(1,3,3-trimethyl-2,3-dihydro-1*H*-2-indolylidenmethyl)-4-(1,3,3-trimethyl-3*H*-2-indoliumylmethylene)-1-cyclobuten-1-olate (**SqCN**): Yield 42%. Dark-green solid. ^{1}H NMR (400 MHz, DMSO-d_6, ppm): δ 7.54 (2H, arom. H, d, J = 7.4 Hz), 7.47–7.37 (4H, arom. H, m), 7.32–7.18 (2H, arom. H, m), 6.30 (2H, C*H*, s), 3.61 (6H, NCH_3, s), 1.68 (12H, (CH_3)$_2$, s). ^{13}C NMR (100 MHz, $CDCl_3$, ppm): δ 173.48, 173.05, 167.94, 167.46, 142.79, 142.07, 128.25, 124.86, 122.39, 119.23, 110.12, 89.21, 49.61, 40.88, 31.82, 26.77. FAB MS, *m/z* calcd. for $[C_{31}H_{28}N_4O]^+$ 472.23, found: 473.2 $[M+H]^+$. Anal. calcd. (%) for $C_{31}H_{28}N_4O$: C, 78.79; H, 5.97; N, 11.86. Found: C, 78.81; H, 5.99; N, 11.85.

3. Results and discussion

3.1. Synthesis

The dyes in this research were chosen in such a way to compare norsquaraines *versus* squaraines of similar structure, and to investigate the effect of substitution in the central squaraine ring on the dye structures and properties. Squaraine **SqO** and its derivatives, where the squaric oxygen is substituted with a barbituric (**SqB**) and a dicyanomethylene (**SqCN**) group, are known to be synthesized by condensation of the quaternized indolenine **2a** with the squaric acid **3a** [40,41] or squarates **3b** and **3c**, respectively [34,40,42] (Scheme 1). Analogous to squaraine **SqO**, norsquaraine **nor-SqO** was obtained starting from indolenine **2b** and squaric acid **3a** [33]. Following this approach, dyes **SqO**, **SqB**, **SqCN**, **nor-SqO** and the new norsquaraines **nor-SqB** and **nor-SqCN** were synthesized. The synthesis was carried out under reflux in a butanol—toluene mixture (1:1, v/v) as proposed in Ref. [42].

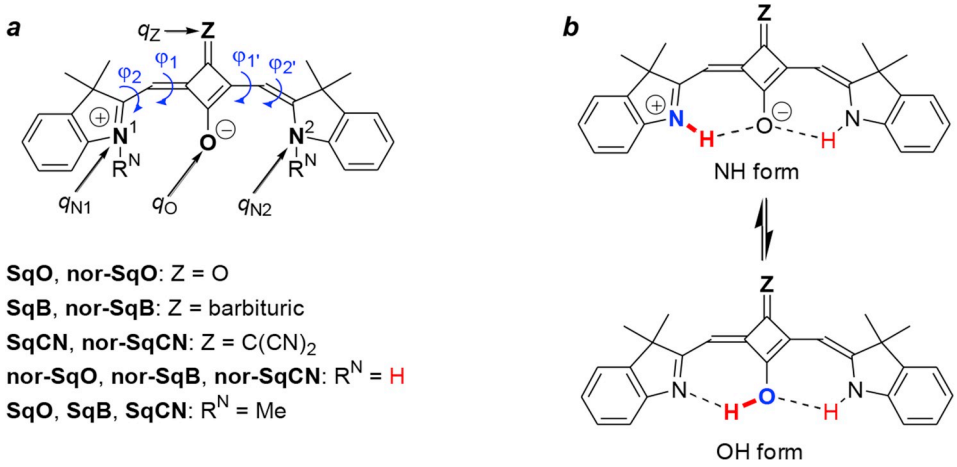

Fig. 1. Internal rotation in the squaraine and norsquaraine molecules (***a***) and potentially possible NH and OH prototropic forms of norsquaraines (***b***).

3.2. Molecular structure

Although nor-squaraines formally differ from squaraines only by the presence of a hydrogen instead of an alkyl substituent at the indolenine nitrogens, their electronic and spatial structures are quite different. Due to internal rotation around the conjugated polymethine bonds (torsion angles φ_1, $\varphi_{1'}$, φ_2, and $\varphi_{2'}$, Fig. 1,a) the squaraine and norsquaraine molecules can potentially exist in different conformational forms. These conformers may have different planarity and different mutual orientation of both indolenine nitrogens relatively to each other (*syn*- and *anti*-forms) and to the squaric oxygens. The indolenine terminal groups can exist in the *cis*- or *trans*-form (rotation around φ_1 and $\varphi_{1'}$) relatively to the central squaric moiety. Furthermore, norsquaraines as compared to squaraines may potentially form two *prototropic* forms (Fig. 1,b), where the hydrogen atom is located either at the indolenine nitrogen (NH form) or the squaraine ring oxygen (OH form). In both prototropic forms, one or two seven-membered quasicycles with an intramolecular H-bond can be formed.

We investigated the molecular structures of norsquaraines **nor-SqO**, **nor-SqB** and **nor-SqCN** *versus* squaraines **SqO**, **SqB** and **SqCN** using experimental (X-ray and NMR) methods and the *ab initio* calculations (B3LYP/6-311G(d,p) method). The calculated total energies (*E*), relative energies (ΔE) (differences in the energies of conformers), populations of the conformers (*c*) at 25 °C, calculated according to the Boltzmann distribution, dipole moments (μ), and electron charges on the indolenine nitrogens (q_{N1}, q_{N2}), squaric oxygen (q_O) and/or substituted squaric oxygen (q_Z) for some typical forms are given in Table S1 (Supplementary data) while the most stable conformers are shown in Table 1 and Fig. 2.

Prototropic forms. The *ab initio* calculations show that the most stable prototropic form of the norsquaraine **nor-SqO** corresponds to the centrosymmetric NH *trans,anti*-form, where both protonated indolenine nitrogens form intermolecular *H*-bonds with two different squaraine oxygens (Table 1). This form is 11.08 kcal/mol and 26.46 kcal/mol more stable than the OH forms with one protonated squaric oxygen and one protonated indolenine nitrogen, and 27.21 kcal/mol more stable compared to the di-OH form (Table S1). Such a difference in the energies suggests that the NH form is the only prototropic form to be realized. These simulations are in good agreement with our X-ray data (Fig. 3,a) showing that **nor-SqO** in crystals exists in the theoretically predicted NH *trans,anti*-form.

X-ray analysis was used also to compare the molecular structure of **nor-SqO** and **SqO** in crystals. Both crystals did not contain solvent molecules, which could affect the molecular conformation as reported in Ref. [31]. Nevertheless, the molecular structure can be distorted by intermolecular interactions in crystals. The obtained data show existence of two halves of **nor-SqO** molecules (**A** and **B**) in the asymmetric part of the unit cell, which is due to both molecules being located in the special positions relatively to the center of symmetry that coincides with the squaraine ring center. The analysis of the bond lengths in **SqO** [43] and **nor-SqO** molecules evidences their mesoionic structures (Table S2, the atom numbering is given in Fig. 3a and b). The N1—C4 bond (1.343–1.354 Å) has ordinary character, which is confirmed by comparison of its value with "standard" mean value for N (3)–Csp^2 bond (1.355 Å) [44]. The value of the C1—O1 bond is very close to the mean value for Csp^2 = O bond (1.210 Å) in **SqO** molecule and it is slightly elongated in **nor-SqO** due to the formation of the N—H···O intramolecular H-bond: NH form, H···O 1.87 Å, N—H···O 158° in **A** and H···O 1.80 Å, N—H···O 157° in **B**. The C1—C2 bond has ordinary character in both dye molecules: the bond length (1.450–1.473 Å) is very close to the mean value for Csp^2–Csp^2 bond (1.455 Å). Pronounced delocalization of the electron density is observed within the C2—C3—C4 chain in both dyes: the C2—C3 and C3—C4 bond lengths (1.371–1.405 Å) are in between the mean values for the Csp^2 = Csp^2 (1.326 Å) and Csp^2–Csp^2 (1.455 Å) bonds.

The analysis of *non-bonded* interactions in the **SqO** crystals reveals a moderate *intramolecular* steric repulsion between the indolenine methyl groups and squaric moiety: the H···C van der Waals radii sum [45] is 2.87 Å as compared to the shortened intramolecular contacts 2.54–2.87 Å (Fig. S1, Table S2). This repulsion is compensated by a slight twisting of the indolenine and squaric moieties relatively to each other (Fig. 3,b). Two parts of **SqO** molecule are nonequivalent due to *intermolecular* interactions in crystals causing also a moderate *non-planarity* of the molecules (the torsion angles are up to 17.1° and the dihedral angles are up to 25.3°). The participation of the methyl group of part **B** in the C—H … π hydrogen bonding with squaric moiety of the neighboring molecule (symmetry operation is 2–x, –y, 1–z; H···C 2.62 Å, C—H···C 133°) causes a more pronounced twisting as compared to part **A** (Fig. 3,b and S1).

In contrast to squaraine **SqO**, the *H*-bonding in norsquaraine **nor-SqO** stabilizes the *planar* geometry (the torsion angle do not exceed 4.9° and the dihedral angles 7.7°). It also causes the elongation of the C1—O1 bond and equalization the C2—C3 and C3—C4 bonds. Thus, the intramolecular and intermolecular steric interactions affect the planar conformation and π-conjugation of squaraine **SqO** [43] in a greater degree than that for norsquaraine **nor-SqO**.

NMR study. The ^{1}H NMR spectrum of **SqO** measured in DMSO-d_6 (Fig. S2,a) and $CDCl_3$ (Fig. S2,b) and the ^{1}H NMR spectrum of **nor-SqO** in DMSO-d_6 (Fig. 4,a) exhibit only one set of peaks. In contrast, the room temperature ^{1}H NMR and ^{13}C NMR spectra of **nor-SqO** in $CDCl_3$ shows two sets of peaks (Fig. 4,b and c). A change in the solvents ratio ($CDCl_3$: DMSO-d_6) causes a change in the relative intensities of these

Table 1
The *ab initio* calculated total energies (*E*), relative energies (Δ*E*), populations of the conformers (*c*) at 25 °C, dipole moments (μ), and electron charges on the indolenine nitrogens (q_{N1}, q_{N2}), squaric oxygen (q_O) and/or substituted squaric oxygen atom (q_Z). The most stable conformers are underlined.

Dye/Form	Conformation	*E*, a.u.	Δ*E*, kcal/mol (*c*, %)	μ, D	q_{N1}, q_{N2}	q_Z, q_O	Torsion angle φ1, φ2 φ1′, φ2′
nor-SqO NH *cis,syn*	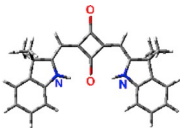	−1265.48611	1.35 (9.0%)	4.18	−0.544 −0.544	−0.745 −0.745	0.0, 0.0, 0.0, 0.0
nor-SqO NH *trans,anti*	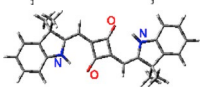	**−1265.48827**	**0.00 (91.0%)**	0.00	−0.543 −0.543	−0.674 −0.674	0.0, 0.0, 0.0, 0.0
SqO *cis,syn(2)*	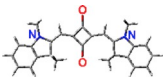	−1344.09204	0.90 (16.75%)	0.49	−0.383 −0.383	−0.635 −0.690	0.0, 0.0, 0.0, 0.0
SqO *trans,anti(1)*	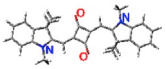	**−1344.09348**	**0.00 (79.04%)**	0.00	−0.383 −0.383	−0.662 −0.662	0.0, 0.0, 0.0, 0.0
SqO *trans,syn*	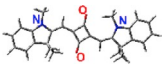	−1344.09074	1.72 (4.08%)	1.39	−0.383 −0.377	−0.660 −0.662	0.1, 0.1, 0.8, 0.3
nor-SqB NH *cis,syn*	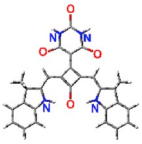	**−1679.23895**	**0.00 (100%)**	7.85	−0.538 −0.538	−0.360 −0.707	−1.1, 0.3, −1.1, 0.3
SqB *cis,syn(2)*	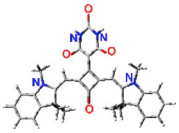	**−1757.84196**	**0.00 (95%)**	5.43	−0.373 −0.373	−0.384 −0.641	−3.1, 6.6, −3.1, 6.7
SqB *cis,anti*	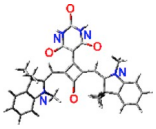	−1757.83912	1.78 (5%)	7.04	−0.373 −0.373	−0.381 −0.640	−23.3, −24.3, 1.2, 4.8
nor-SqCN NH *cis,syn*	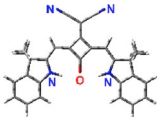	**−1414.07885**	**0.00 (100%)**	10.21	−0.536 −0.536	−0.396 −0.713	0.0, 0.0, 0.0, 0.0
SqCN *cis,syn*	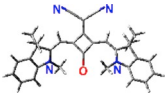	**−1492.67819**	**0.00 (100%)**	10.12	−0.372 −0.372	−0.420 −0.650	−14.6, −20.9, −14.6, −20.9

two sets (Fig. 4,d). However, the addition of an equimolar amount of one solvent to a dye dissolved in the other solvent has almost no effect on the spectra evidencing that the above phenomenon is not connected with the specific interaction between the dye and the solvent molecules but is just due to the general solvent effect.

The two sets of peaks (Fig. 4,b) in the ^{1}H NMR spectrum of **nor-SqO** in $CDCl_3$ belong to two conformers at a ratio of 2:1. Both conformers have a symmetrical structure as evidenced by the presence of only one set of peaks for the methine CH, indolenine NH and 3-$(CH_3)_2$ hydrogens. These conformers have intramolecular hydrogen bonds with a low field chemical shift of the NH hydrogen at δ = 12.84 ppm for the *trans,anti*-form and δ = 12.54 ppm for the *cis,syn*-form. Only two structures of the four possible symmetrical forms shown in Fig. 5, **nor-SqO** NH *trans, anti* and **nor-SqO** NH *cis,syn*, have intramolecular hydrogen bonds.

Also the ^{1}H−^{1}H NOESY supports the coexistence of these two conformers, confirming that the hydrogens of the 3-$(CH_3)_2$ and the methine CH groups in both conformers are in close proximity to each other and therefore cross peaks are seen in the 2D-NOESY experiment. **Nor-SqO** NH *trans, anti* has a cross peak between δ = 1.45 ppm (3-$(CH_3)_2$) and δ = 5.48 ppm (C*H*) and **nor-SqO** NH *cis,syn* has a cross peak between δ = 1.45 ppm (3-$(CH_3)_2$ hydrogens) and δ = 5.52 ppm (C*H*) (Fig. S3,a).

The two conformers can be distinguished using ^{13}C NMR spectroscopy (Fig. 4,c and S4). The **nor-SqO** NH *trans, anti* has C_2 symmetry (Fig. 5); each squarate oxygen forms one intra-molecular H-bond with the NH hydrogen and the chemical shift of the carbon is 183.42 ppm. In contrast, **nor-SqO** NH *cis,syn* has a σ_2 symmetry and thus the two oxygens are different. One oxygen forms two intramolecular *H*-bonds and the chemical shift of the carbon is 185.59 ppm while the other oxygen is lacking a *H*-bond and the chemical shift of the carbon is observed at a higher field, δ = 180.31 ppm.

The one bond coupling constants ($^1J_{N\text{-}H}$) between the ^{15}N and ^{1}H of the two conformers were extracted from the 2D experiment HMBC ^{15}N−^{1}H (Fig. S3,b) and their values are almost the same: 92 Hz and 94 Hz for the major and the minor conformers, respectively. These values confirm that in solution the hydrogen atom is also bound to the nitrogen atom as predicted by *ab initio* simulation.

When the ^{1}H NMR spectrum of **nor-SqO** in $CDCl_3$ (Fig. 4,b), is

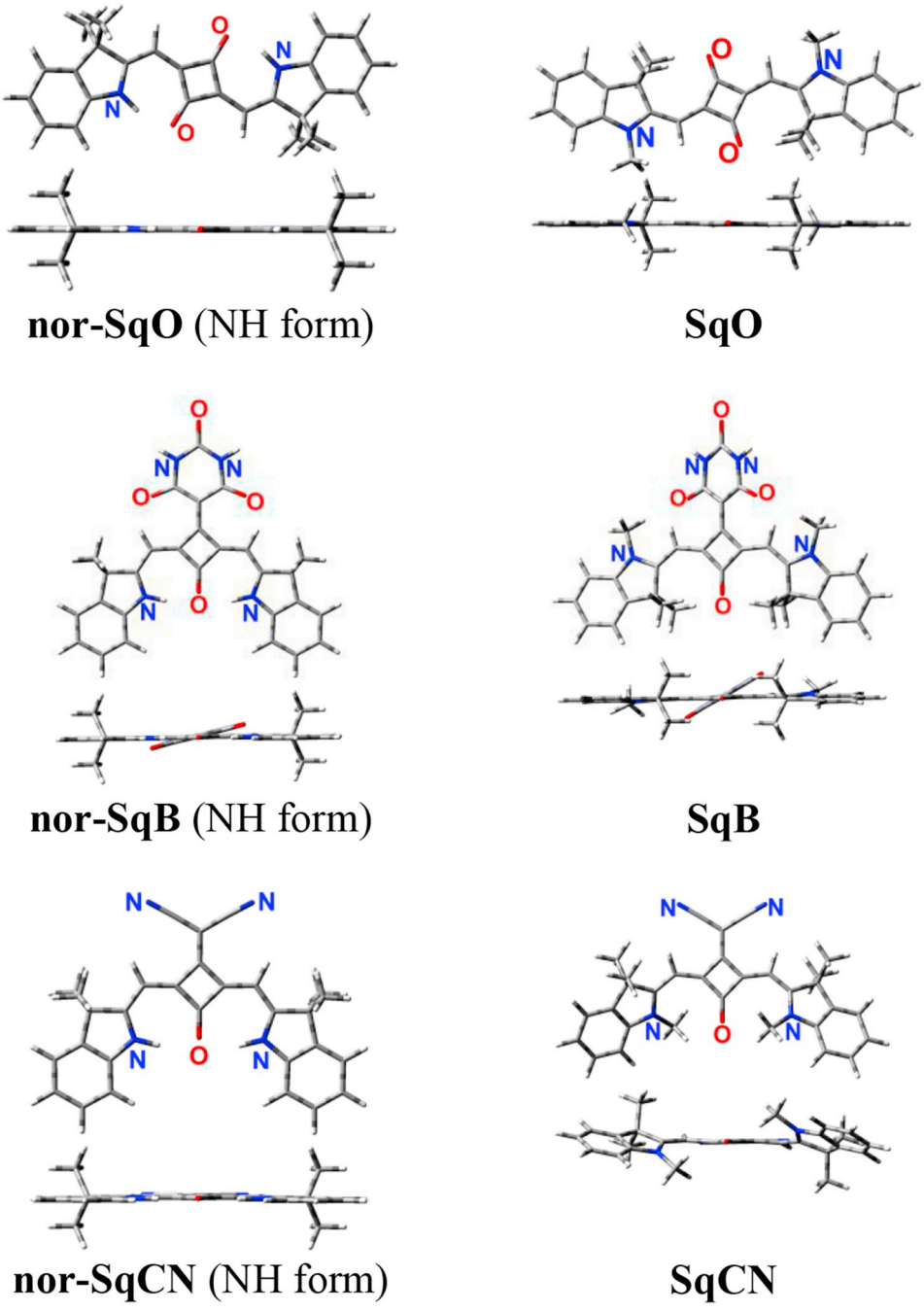

Fig. 2. The most stable conformers of squaraine and norsquaraine molecules according to the *ab initio* simulations.

compared to the spectrum in DMSO-d_6, at room temperature, the latter one shows only one set of broad peaks (Fig. 4,a). A series of ^{1}H NMR experiments at high temperatures (330–370 K) displays a narrowing of some of the peaks as we increase the temperature. For example, the line width of the methine hydrogen (CH) is decreasing from 4.86 Hz at 300 K to 0.8 Hz at 370 K (Fig. S5). These observations suggest that the two conformers, NH *trans, anti* and NH *cis,syn,* are both present in DMSO-d_6 and the equilibrium is rapid in the NMR time scale at room temperature to be above the coalesce but not fully narrow. Further, most of the ^{13}C signals are broad at room temperature (Fig. S4) and the carbonyl signal is very broad, so it disappears in the spectrum noise. This equilibrium is obviously slow in the NMR time scale when the compound is dissolved in $CDCl_3$ to yield two sets of peaks.

Conformations. *Ab initio* simulations indicate that norsquaraine **nor-SqO** exists mostly in the centrosymmetric *trans,anti*-form with an insufficient contribution of *cis,syn*-form, which is 1.35 kcal/mol less stable (Table 1 and S1, Fig. 5). According to the Boltzmann distribution the ratio between these forms at 25 °C is about 91% : 9%. This is in good agreement with data reported in Ref. [32], where *trans,anti*-form was found to be 0.5 kcal/mol less stable compared to *cis,syn*-form. The most stable *trans,anti*-form of **nor-SqO** is realized in crystals (Fig. 3,a, Table 1). However, due to the ΔE between these conformers is not pronounced it is anticipated that *trans,anti*- and *cis,syn*-forms of **nor-SqO** and **SqO** can coexist in solutions.

Similar to **nor-SqO**, the squaraine molecule **SqO** can also exist in different conformations (Table 1 and S1). The most stable conformer of **SqO** is also centrosymmetric; it has a *trans*-orientation of indolenine moieties and *anti*-orientation of indolenine nitrogens (Fig. 2). However, the calculated energy of this form is only about 0.90 kcal/mol lower compared to that of the *cis,syn*-form and 1.72 kcal/mol lower than that

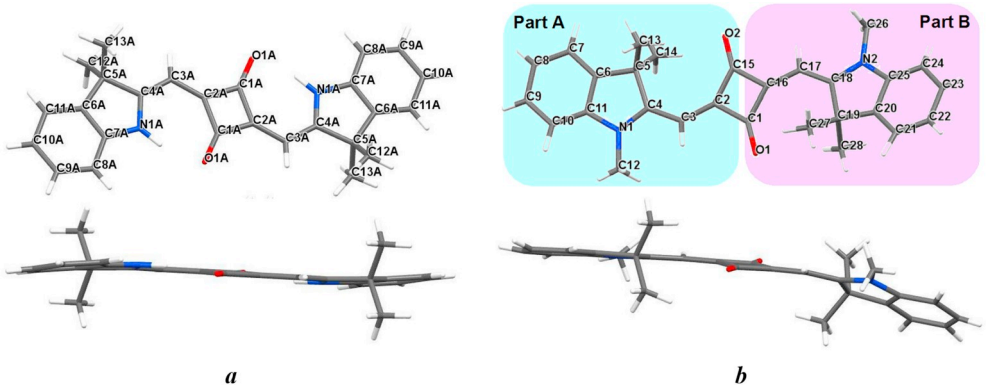

Fig. 3. The **nor-SqO** (***a***) and **SqO** (***b***) structures according to the X-ray data.

of the *trans,syn*-form (Table 1). According to the Boltzmann distribution the ratio between these forms at 25 °C is about 79%: 17%: 4%, respectively. The contribution of other conformers is only minor (< 0.2%). The most stable theoretically predicted *trans, anti(1)* conformer is realized in crystals (Fig. 3,b) [43].

Planarity. *Ab initio* calculations show that both **SqO** and **nor-SqO** molecules are flat (φ_1, φ_2, $\varphi_{1'}$, $\varphi_{2'} \approx 0°$). The planarity of **nor-SqO** was found to be in good agreement with X-ray data (Fig. 3,a). However the planarity of **SqO** in crystals (Fig. 3,b) is somewhat disrupted ($\varphi_1 = +2.8°$, $\varphi_2 = +7.0°$, $\varphi_{1'} = -7.8°$, $\varphi_{2'} = -17.1°$, torsion angles are designated in Fig. 1) [43]. The non-planarity of **SqO** in crystals is rather due to the above mentioned *inter*-molecular interactions in the crystal phase (Fig. S1, Table S2) than of *intra*-molecular sterical hindrance caused by the indolenine N-methyl groups.

Substitution of squaric oxygen. Similar to **nor-SqO**, barbituric (**nor-SqB**) and dicyanomethylene (**nor-SqCN**) norsquaraines according to *ab initio* calculations also exist entirely in the **NH** forms (Table 1 and S1). Substitution of the squaric acid oxygen with these rather bulky groups has a strong impact on the conformations of the squaraine and norsquaraine molecules. The calculations show that **SqB**, **nor-SqB**, **SqCN**, and **nor-SqCN** exceptionally have a *cis*-orientation of indolenine moieties and a *syn*-orientation of the indolenine nitrogens (Fig. 2). These simulations are in good agreement with the ^{1}H NMR data exhibiting only one set of peaks for these dyes. The nitrogen atoms are located on the same side as the squaric oxygen. The exception is squaraine **SqB**, where the nitrogen atoms are on the same side as the barbituric moiety.

In contrast to oxosquaraine **SqO**, barbituric (**SqB**) and especially dicyanomethylene (**SqCN**) squaraines are less planar (see torsion angles in Table 1). At the same time, norsquaraines **nor-SqB** and **nor-SqCN** as well as **nor-SqO** are very flat.

Similar to **nor-SqO**, the intramolecular *H*-bonds between the indolenine NH hydrogens and squaric acid oxygen are realized also in the **nor-SqB** and **nor-SqCN** molecules. However, in contrast to **nor-SqO**, these *H*-bonds are formed with the same squarate oxygen atom, so that the molecules have a mirror-symmetrical structure. In the **SqB** and **nor-SqB** the barbituric oxygens form additional *H*-bonds with the methine hydrogens.

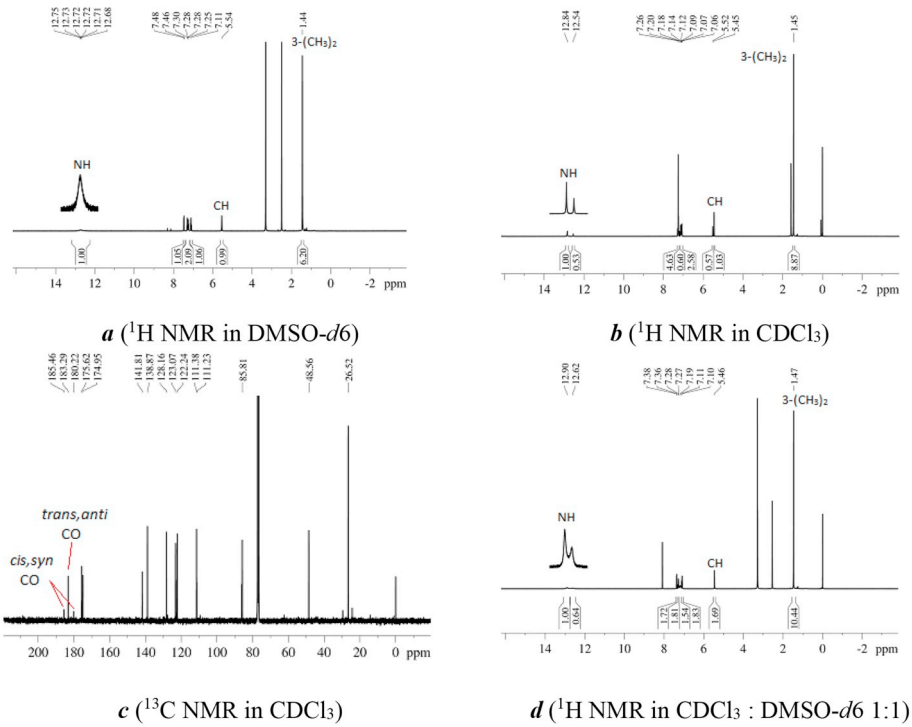

a (^{1}H NMR in DMSO-*d6*) ***b*** (^{1}H NMR in $CDCl_3$)

c (^{13}C NMR in $CDCl_3$) ***d*** (^{1}H NMR in $CDCl_3$: DMSO-*d6* 1:1)

Fig. 4. ^{1}H NMR (***a,b,d***) and ^{13}C NMR (***c***) spectra of norsquaraine **nor-SqO** in DMSO-d_6 (***a***), $CDCl_3$ (***b, c***) and $CDCl_3$: DMSO-d_6 1:1 (***d***).

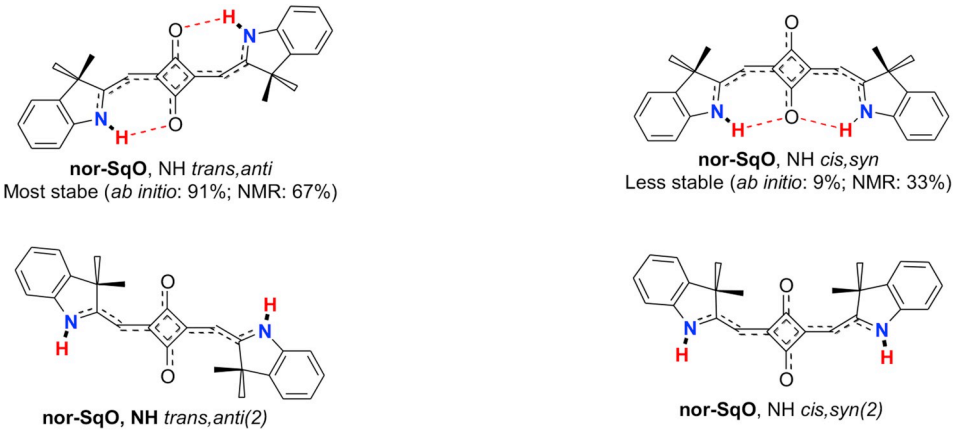

Fig. 5. Symmetrical forms of **nor-SqO**.

The intramolecular *H*-bonds facilitate flattening but also increase the conformational rigidity of the norsquaraine molecules (Fig. 3,a) as compared to squaraines (Fig. 3,b). Thus, the calculations show that the rotation barrier associated with torsion angle φ_1 in the **nor-SqO** molecule is about 26.1 kcal/mol, whereas in the **SqO** molecule it is substantially less pronounced, 18.3 kcal/mol. The rotation barriers associated with torsion angle φ_2 are higher (33.6 kcal/mol and 24.0 kcal/mol, respectively).

Electron density distribution. Both squaraine and norsquaraine chromophores are neutral and have a zwitter-ionic structure. The electronic charge in all these molecules is delocalized mostly within the polymethine chain (Table S3). The calculations exhibit a negative charge on the squaric oxygen (q_O) and a less pronounced charge on the indolenine nitrogens (q_{N1}, q_{N2}) and on the carbon of the substituted squaric oxygens (q_Z) (Table 1). The positive charge is mostly on the squaric "carbonyl" carbons and on the indolenine carbons at the position 2.

The most stable conformers of squaraine **SqO** and norsquaraine **nor-SqO** are centrosymmetric; $q_O = q_Z$, $q_{N1} = q_{N2}$ and therefore the molecular dipole moments (μ) are about zero. While the negative charges on the oxygens (q_O, q_Z) in **SqO** and **nor-SqO** are almost equal (-0.66 and -0.67, respectively), the charges on the **nor-SqO** nitrogens (q_{N1}, q_{N2}) are greatly increased as compared to **SqO** (-0.54 *vs.* -0.38).

Substitution of the oxygen atom in **SqO** and **nor-SqO** with barbituric (**SqB** and **nor-SqB**) and dicyanomethylene (**SqCN** and **nor-SqCN**) groups causes a noticeable increase in the calculated dipole moments (μ) which increases in the order of **SqO** (0 D) = **nor-SqO** (0 D) ≪ **SqB** (5.43 D) < **nor-SqB** (7.85 D) < **SqCN** (10.12 D) ≈ **nor-SqCN** (10.21 D).

Molecular structure of norsquaraines versus squaraines. Squaraines and norsquaraines have similar molecular structure, electronic density distribution and dipole moments but norsquaraines have an increased "local" polarity expressed by the increased electron charges on the indolenine nitrogens as compared to those of squaraines. In addition, norsquaraine molecules contain intramolecular *H*-bonds and therefore they are conformationally more rigid and more planar.

3.3. Spectral properties

3.3.1. Dyes free in solutions

The absorption and emission maxima (λ_{max}), molar absorptivities (ε), quantum yields (Φ_F), Stokes shifts ($\Delta\nu_{st}$), and spectral band half-widths ($\Delta\nu_{1/2}$) of norsquaraine dyes measured free in solutions and after non-covalent binding to protein (BSA), are summarized in Table 2.

The absorption spectra of norsquaraine **nor-SqO** and squaraine **SqO**, measured in $CHCl_3$ consist of only one long-wavelength band with a molar absorptivityý ε = 218,000 $M^{-1}cm^{-1}$ and 219,000 $M^{-1}cm^{-1}$, respectively.

Substitution of squaric oxygen in both **SqO** and **nor-SqO** molecules with the barbituric moiety (**SqB**, **nor-SqB**) causes a 6–27 nm red-shift of the absorption and emission bands (Table 2). Introduction of the dicyanomethylene group (**SqCN**, **nor-SqCN**) results in a more pronounced red-shift (20–60 nm). Dyes **SqB**, **nor-SqB**, **SqCN**, **nor-SqCN** as compared to **SqO** and **nor-SqO** exhibit an additional, short-wavelength absorption band at 427–441 nm (barbituric) and 381–388 nm (dicyanomethylene) with molar absorptivity (ε) of up to 35,000 $M^{-1}cm^{-1}$, which makes them suitable for excitation within the blue/UV spectral range (Fig. 6).

The ***absorption and emission bands*** of norsquaraines are in the long-wavelength range of 654–694 nm and 669–712 nm, respectively. These bands are 11–28 nm red-shifted as compared to the corresponding squaraines **SqO**, **SqB** and **SqCN** (Table 2), which is more likely due to their more planar molecular structure. The main absorption spectra of squaraines and norsquaraines consist of an intense, long-wavelength band and a less intense shoulder on the shorter-wavelength slope of the main band (Fig. 6). This sholder is typical for cyanines and squaraines and known to belong to a vibronic mode [19].

While the absorption bands of the investigated squaraines and norsquaraines measured in $CHCl_3$ do not exhibit any sign of aggregation, these dyes do strongly aggregate in aqueous media. The extinction coefficients measured in $CHCl_3$ significantly decrease in PB pH 7.4 — DMSO (5:1, v/v) and a pronounced aggregation band appears on the shorter-wavelength slope of the absorption band (Fig. 7,a–f). The aggregation band of cyanines and squaraines is known to be located very close to the vibronic shoulder [46]. Barbituric, dicyanomethylene squaraines and norsquaraines exhibit more pronounced aggregation than **SqO** and **nor-SqO**. The level of aggregation for the dye pairs **SqO**/**nor-SqO** and **SqCN**/**nor-SqCN** seems very similar while for **nor-SqB** it is higher compared to **SqB**.

It is worth mentioning that the investigated dyes have reduced solubility not only in aqueous media but also in $CHCl_3$ and DMSO. As a result, we were unable to measure ^{13}C NMR spectra of **SqB** and **nor-SqB** in $CDCl_3$ and DMSO.

The Stokes shifts ($\Delta\nu_{st}$) for norsquaraines and squaraines in $CHCl_3$ increase in the order: oxo < dicyanomethylene < barbituric (Table 2), while the molecular polarity represented by the dipole moment increases in the order: oxo < barbituric < dicyanomethylene. The increased $\Delta\nu_{st}$ of barbituric and dicyanomethylene derivatives as compared to **SqO** and **nor-SqO** is more likely due to their more polar structure. The substantially increased $\Delta\nu_{st}$ of **SqB** and **nor-SqB** as compared to other derivatives is supposedly due to the change in the intramolecular *H*-bonds between barbituric oxygens and methine hydrogens in the excited state. The intramolecular *H*-bonds cause a decrease in the molar absorptivities of barbituric derivatives compared to other dyes. Interestingly, the Stokes shifts ($\Delta\nu_{st}$) and the spectral band half-widths ($\Delta\nu_{1/2}$) for **nor-SqO** in $CHCl_3$ are higher than those of **SqO**

Table 2
Spectral characteristics of free dyes (c_{Dye} ~ 0.5 μM) and their complexes with 90 μM BSA at T = 25°C.

Dye	Media	λ_{max} (Ab), nm	λ_{max} (Em), nm	ε, $M^{-1}cm^{-1}$	Φ_F, %	$\Delta\nu_{st}$, cm^{-1}	$\Delta\nu_{1/2}$ (Ab), cm^{-1}	$\Delta\nu_{1/2}$ (Em), cm^{-1}
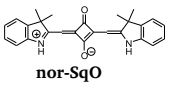 **nor-SqO**	$CHCl_3$	654	669	218,000	45	340	780	730
	MeOH	647	662	200,000	44	350	830	800
	DMF	657	673	206,000	45	360	820	770
	DMSO	659	678	219,000	43	430	840	780
	DMSO—$CHCl_3$ (1:1)	658	675	215,000	47	380	790	770
	DMF—water (1:1)	647	666	n/d	29	440	870	790
	PB pH 7.4—DMSO (5:1)	639	659	92,000	13	470	960	850
	BSA-Complex PB pH 7.4	655	669	200,000	36	320	870	890
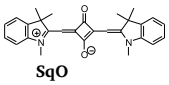 **SqO**	$CHCl_3$	633	642	219,000	25	220	690	690
	MeOH	625	635	n/d	4	250	640	690
	DMSO	641	652	n/d	15	260	660	650
	PB pH 7.4—DMSO (5:1)	624	635	n/d	3	280	750	740
	BSA-Complex PB pH 7.4	639	645	203,000	44	150	670	670
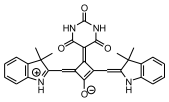 **nor-SqB**	$CHCl_3$	669	693	63,000	48	520	980	830
		441		16,000				
	PB pH 7.4—DMSO (5:1)	673	n/a[a]	n/a[a]	< 1	n/a[a]	n/a[a]	n/a[a]
	BSA-Complex PB pH 7.4	662	683	23,000	9	460	2270	980
		460		15,000				
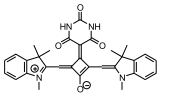 **SqB**	$CHCl_3$	641	669	103,000	4	650	1110	1380
		427		27,000				
	PB pH 7.4—DMSO (5:1)	618	646	86,000	< 1	700	1410	1620
		426		23,000				
	BSA-Complex PB pH 7.4	633	657	91,000	34	580	1180	1540
		422		13,000				
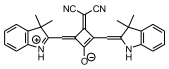 **nor-SqCN**	$CHCl_3$	694	712	120,000	28	360	750	730
		388		33,000				
	PB pH 7.4—DMSO (5:1)	698	n/a[a]	28,000	< 1	n/a[a]	n/a[a]	n/a[a]
		389		19,000				
	BSA-Complex PB pH 7.4	690	704	63,000	13	290	1730	830
		394		32,000				
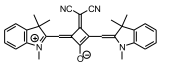 **SqCN**	$CHCl_3$	683	701	196,000	37	380	800	830
		381		35,000				
	PB pH 7.4—DMSO (5:1)	660	678	70,000	< 1	400	2030	1510
		384		16,000				
	BSA-Complex PB pH 7.4	682	702	162,000	50	420	830	850
		380		36,000				

[a] Not available because of the low solubility and/or high aggregation.

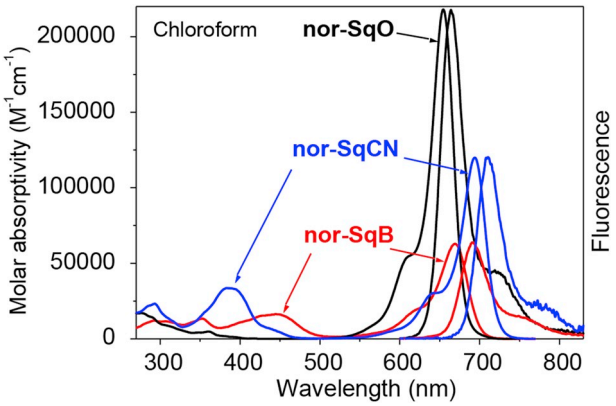

Fig. 6. Absorption and emission spectra of **nor-SqO**, **nor-SqB** and **nor-SqCN** measured in $CHCl_3$.

while for the dye pairs **nor-SqB/SqB** and **nor-SqCN/SqCN** an opposite correlation is observed. For norsquaraines $\Delta\nu_{1/2}$(Ab) > $\Delta\nu_{1/2}$(Em), while for **SqO** they are almost the same and for **SqB** and **SqCN** $\Delta\nu_{1/2}$(Ab) < $\Delta\nu_{1/2}$(Em). Both $\Delta\nu_{st}$ and $\Delta\nu_{1/2}$ increase, when $CHCl_3$ is replaced with water, which is typical for polar dyes.

The quantum yields (Φ_F) of norsquaraines **nor-SqO** and **nor-SqB** measured in $CHCl_3$ are 1.8 and 12 fold higher compared to **SqO** and **SqB** while for **nor-SqCN** the Φ_F is surprisingly 1.3 times lower.

The quantum yields of *squaraine* dyes are known to be strongly affected by the solvent polarity [47,48]. The Φ_F of **SqO**, **SqB** and **SqCN** substantially increases, when a polar solvent such as water, alcohol or DMSO is substituted with a less polar solvent such as $CHCl_3$ (Table 2). For instance, the quantum yield of **SqO** in $CHCl_3$ (Φ_F = 25%) is 8 fold decreased in PB pH 7.4 — DMSO (5:1) (Φ_F = 3%) and 6 fold in MeOH (Φ_F = 4%).

In contrast, the solvent polarity has a marginal effect on the quantum yield of *norsquaraines*. The quantum yield of **nor-SqO** in DMSO (Φ_F = 43%), DMF (Φ_F = 45%) and MeOH (Φ_F = 44%) is almost the same as in the less polar solvent $CHCl_3$ (Φ_F = 45%) and DMSO—$CHCl_3$ (1:1, v/v) (Φ_F = 47%) (Table 2). At the same time, the Φ_F of **nor-SqO** measured in DMSO or DMF decreases upon dilution with water. Thus, the Φ_F is 43% in DMSO and 45% in DMF while it is only 29% in water—DMSO or water—DMF (1:1, v/v) and 13% in PB pH 7.4—DMSO (5:1). The quantum yield decrease in aqueous media can be attributed to the aggregation of **nor-SqO** molecules. This is evidenced by the increase in the aggregation band at the short-wavelength slope of the main absorption band (around 600 nm) and the decrease in the main band (around 650 nm) (Fig. 8,a). Furthermore, upon increasing the water ratio to more then about 40:1 (v/v), an additional aggregation band appears at the long-wavelength slope of the main absorption band (at about 700 nm).

In case of **SqCN**, **nor-SqCN** and especially **SqB** and **nor-SqB**, the aggregation noticeably increases causing a dramatic decrease in the quantum yields: Φ_F < 1% in PB pH 7.4 — DMSO (5:1, v/v) (Table 2).

As shown above, the ^{1}H NMR and ^{13}C NMR spectra of **nor-SqO**, measured in $CDCl_3$ as compared to DMSO-d_6, contain two groups of signals, which is due to coexistence of two conformers. However, the absorption spectra measured in $CHCl_3$, MeOH, DMF, and DMSO contain only one band (Fig. 8,b). This suggests that the above conformers have similar spectral properties. The solvent causes a slight red-shift in the

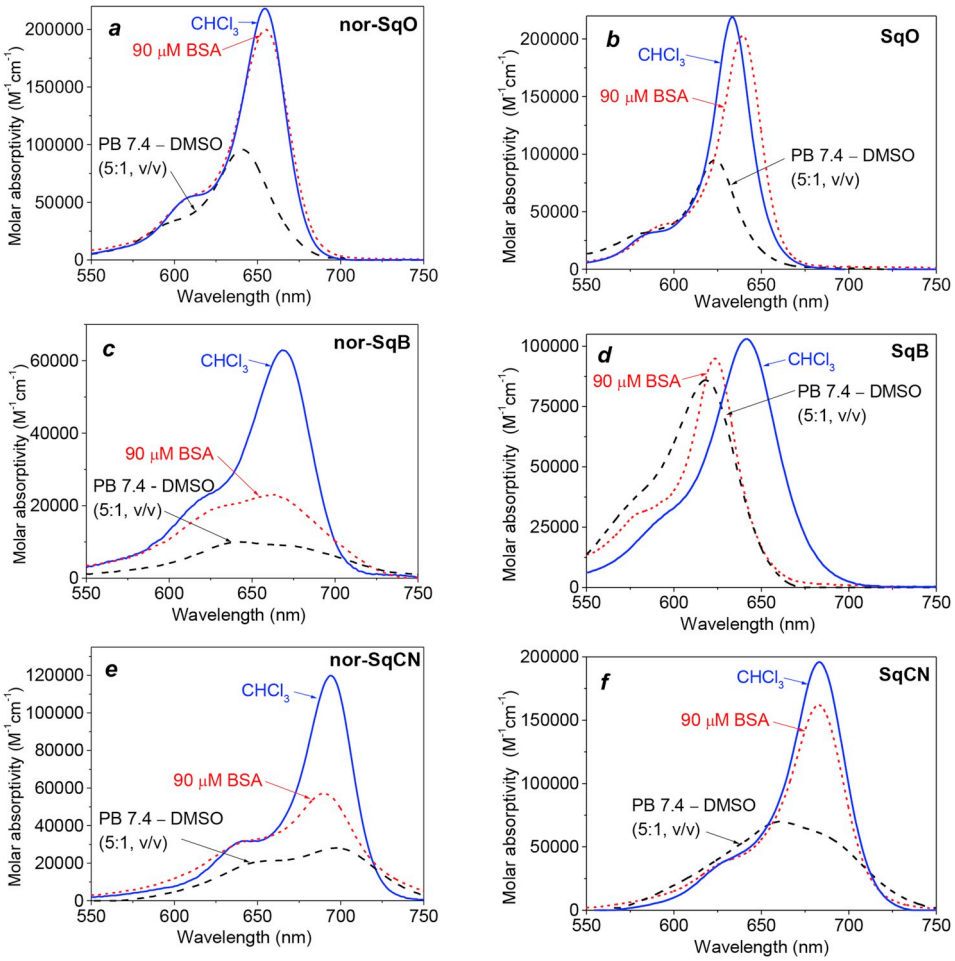

Fig. 7. Absorption spectra of norsquaraines and squaraines in $CHCl_3$ and PB pH 7.4 in presence of DMSO (5:1, v/v) and 90 μM BSA.

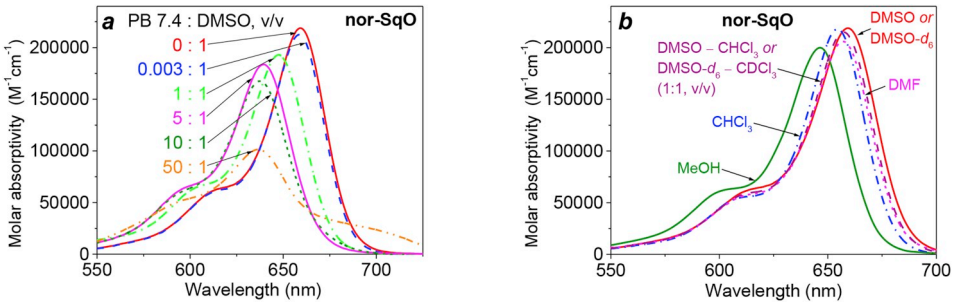

Fig. 8. Absorption spectra of **nor-SqO** (c_{dye} = 0.5 μM) in PB 7.4 — DMSO mixtures (***a***) and in different solvents (***b***).

nor-SqO spectra and this shift increases in the order of PB–DMSO (5:1) < MeOH < $CHCl_3$ < DMF < DMSO while the molar absorptivity remain almost unchanged (Table 2).

3.3.2. *Non-covalent complexation with BSA*

The absorption and emission spectra and the quantum yields of *squaraines* measured in aqueous buffers are known to be substantially affected by the presence of proteins in particular bovine serum albumin (BSA), which is due to the formation of dye—BSA complexes: there is a moderate red-shift and noticeable increase in the quantum yield [42,49]. These effects have been explained by decrease in the environment polarity [46,50] and increase in the conformational rigidity [51] of dye molecules, when they move from water to protein phase.

We found that the spectral properties of *norsquaraines* also do change in the presence of BSA (Fig. S6,a,b). For both investigated dye classes, squaraines and norsquaraines, measured at c_{Dye} = 0.5 μM these characteristics reach "saturation" when the concentration of BSA reaches c_{BSA} ~ 90 μM and then do not change anymore. Therefore, the spectral characteristics of the dye—BSA complexes presented in Table 2 were measured at c_{BSA} = 90 μM.

When compared to PB pH 7.4 upon complexation with BSA *squaraines* **SqO** and **SqB** — DMSO (5:1, v/v) exhibit an about 15/10 nm red-shift of the absorption/emission bands and **SqCN** shows a 22/24 nm red-shift. *Norsquaraine* **nor-SqO** in presence of BSA also shows about the same *red*-shift (16/10 nm) as **SqO** while **nor-SqB** and **nor-SqCN** exhibit ~10 nm *blue*-shift, which is more likely due to their higher polarity.

In general, the Stokes shifts of squaraines and norsquaraines (except **SqCN**) in aqueous BSA are shorter compared to $CHCl_3$, which is most likely due to the more viscous protein environment.

The fluorescence intensities of *squaraines* measured in aqueous media (PB pH 7.4 — DMSO, 5:1, v/v) dramatically increase in presence of BSA (Fig. S6,b). The quantum yields (Φ_F) increase by factors of ~15, > 34, and > 50, respectively (Table 2). It was difficult to determine the accurate values of these increases for **SqB** and **SqCN** because of the extremely low Φ_F in PB pH 7.4 — DMSO (5:1, v/v). Importantly, the Φ_F of *norsquaraine* **nor-SqO** increases only by factor of 2.8 (as compared to 15 fold for **SqO**), while in the absence of BSA it is higher compared to **SqO** (Table 2, Fig. S6,a). Thus, **nor-SqO** is less sensitive to BSA than **SqO**, which can be attributed to its more rigid structure. **Nor-SqB** and **nor-SqCN** demonstrate a substantially more pronounced increases in the Φ_F (> 9 and > 13), which is most likely due to a higher polar structure of these molecules (higher dipole moments, Table 1).

The increase in the quantum yields of the investigated squaraines and norsquaraines in the presence of BSA is supposedly not only due to the decrease in the environment *polarity* and increase in the conformational *rigidity* of these dye molecules but also because of the decrease in their *aggregation*. The decrease in aggregation can be seen from the decrease of the aggregation band (Fig. 7a–f) and increase in the extinction coefficients (Table 2).

The quantum yields of BSA complexes of norsquaraines are lower than those for squaraines: 36/44% for **nor-SqO/SqO**, 9/34% for **nor-SqB/SqB**, and 13/50% for **nor-SqCN/SqCN**. This correlation is also in good agreement with the aggregation ability of these dyes: While **nor-SqO** and **SqO** in BSA exhibit an insufficient tendency to aggregate (Fig. 7a and b), **nor-SqCN** (Fig. 7,e) and especially **nor-SqB** (Fig. 7,c) demonstrate a much more pronounced aggregation tendency compared to **SqCN** (Fig. 7,f) and **SqB** (Fig. 7,d).

4. Conclusions

In summary, we have synthesized the indolenine based norsquaraine dye **nor-SqO** and its novel barbituric (**nor-SqB**) and dicyanomethylene (**nor-SqCN**) derivatives; investigated their molecular structures, spectral properties and complexation with BSA *versus* those of conventional squaraines of similar structures (**SqO**, **SqB** and **SqCN**). Due to the intramolecular *H*-bonds, norsquaraine molecules are more planar and rigid compared to squaraines, and have therefore higher fluorescence quantum yields in solutions. In solution norsquaraine **nor-SqO** exists as a mixture of two conformers, where the non-polar centrosymmetric one is dominant. In contrast, barbituric and dicyanomethylene squaraines and norsquaraines are highly polar. Due to the more rigid structure and lower polarity, the quantum yield of **nor-SqO** is less sensitive to the presence of protein (BSA) than **SqO**. This suggests that **nor-SqO** might be useful for biomedical assays based on a specific interaction of the dye—biomolecule conjugates with biological counterparts (antibody—antigen, biotin—avidin, complimentary oligonucleotides, and receptor—ligand interactions) in heterogeneous biological media, where the presence of non-targeting proteins and other large-molecular-weight biomolecules could affect the assay. At the same time, highly polar norsquaraines **nor-SqB** and **nor-SqCN** as well as squaraines **SqO**, **SqB** and **SqCN** might be promising fluorescent probes for sensing applications in proteins and other high-molecular-weight species.

Acknowledgements

The work was supported by the Science and Technology Center in Ukraine (STCU, project P548, SETA BioMedicals), the National Academy of Sciences of Ukraine (projects 0116U001210 and 0117U001281) and Program of Fundamental Research "New Functional Substances and Materials for Chemical Engineering" (project 0117U005088). Leonid Patsenker is thankful to the Center for Absorption in Science of the Ministry of Immigrant Absorption of Israel for the financial support under the KAMEA program. The authors are grateful to Dr. Illia Serdiuk (Gdansk University) for the measurements of mass-spectra and Dr. Hugo Gottlieb (Bar Ilan University, Israel) for helpful discussion on NMR results.

Appendix A. Supplementary data

Supplementary data to this article can be found online at https://doi.org/10.1016/j.dyepig.2018.12.007.

References

[1] Geddes CD. Reviews in fluorescence 2016, Reviews in fluorescence. Springer; 2017https://doi.org/10.1007/978-3-319-48260-6.
[2] Friães S, Silva AM, Boto RE, Ferreira D, Fernandes JR, Souto EB, Almeida P, Ferreira LFV, Reis LV. Synthesis, spectroscopic characterization and biological evaluation of unsymmetrical aminosquarylium cyanine dyes. Bioorg Med Chem 2017;25:3803–14https://doi.org/10.1016/j.bmc.2017.05.022.
[3] Tatikolov AS, Panova IG, Ishchenko AA, Kudinova MA. Spectral and fluorescent study of the interaction of squarylium dyes, derivatives of 3*H*-indolium, with albumins. Biophysics 2010;55:35–40https://doi.org/10.1134/S0006350910010070.
[4] Haugland RG. The molecular probes handbook: A guide to fluorescent probes and labeling technologies. Life Technologies Corporation; 2010.
[5] Brahme A. Comprehensive biomedical physics. Elsevier Science; 2014.
[6] Escobedo JO, Rusin O, Lim S, Strongin RM. NIR dyes for bioimaging applications. Curr Opin Chem Biol 2010;14:64–70https://doi.org/10.1016/j.cbpa.2009.10.022.
[7] Narayanaswamy R, Wolfbeis OS. Optical sensors: Industrial environmental and diagnostic applications. Springer Series on Chemical Sensors and Biosensors. Berlin, Heidelberg: Springer; 2014.
[8] Luo Sh, Zhang E, Su Y, Cheng T, Shi Ch. A review of NIR dyes in cancer targeting and imaging. Biomaterials 2011;32:7127–38https://doi.org/10.1016/j.biomaterials.2011.06.024.
[9] Anees P, Joseph J, Sreejith S, Menon NV, Kang Y, Yu WK, Ajayaghosh A, Zhao Y. Real time monitoring of aminothiol level in blood using a near-infrared dye assisted deep tissue fluorescence and photoacoustic bimodal imaging. Chem Sci 2016;7:4110–6https://doi.org/10.1039/c5sc04986e.
[10] Patsenker LD, Tatarets AL, Klochko OP, Terpetschnig EA. Conjugates, complexes, and interlocked systems based on squaraines and cyanines. In: Demchenko A, editor. Advanced fluorescence reporters in chemistry and biology II. Springer Series on Fluorescence (Methods and Applications). vol. 9. Berlin, Heidelberg: Springer; 2010. p. 159–90https://doi.org/10.1007/978-3-642-04701-5_5.
[11] Paynea A-Jo, Welch GC. Optimized synthesis of π-extended squaraine dyes relevant to organic electronics by direct (hetero)arylation and Sonogashira coupling reactions. Org Biomol Chem 2017;15:3310–9https://doi.org/10.1039/C7OB00362E.
[12] Paternò GM, Barbero N, Galliano S, Barolo C, Lanzani G, Scotognella F, Borrelli R. Excited state photophysics of squaraine dyes for photovoltaic applications: an alternative deactivation scenario. J Mater Chem C 2018;6:2778–85https://doi.org/10.1039/C7TC05078J.
[13] Chan S, Bantang JP, Camacho D. Influence of nanomaterial fillers in biopolymer electrolyte system for squaraine-based dye-sensitized solar cells. Int J Electrochem Sci 2015;10:7696–706.
[14] Mayerhöffer U, Gsänger M, Stolte M, Fimmel B, Würthner F. Synthesis and molecular properties of acceptor-substituted squaraine dyes. Chem Eur J 2013;19:218–32. https://doi.org/10.1002/chem.201202783.
[15] Lynch DE, Kirkham AN, Chowdhury MZH, Wane ES, Heptinstall J. Water soluble squaraine dyes for use as colorimetric stains in gel electrophoresis. Dyes Pigments 2012;94:393–402https://doi.org/10.1016/j.dyepig.2012.02.001.
[16] de Miguel G, Marchena M, Zitnan M, Pandey SS, Hayase S, Douhal A. Femto to millisecond observations of indole-based squaraine molecules photodynamics in solution. Phys Chem Chem Phys 2012;14:1796–805https://doi.org/10.1039/C1CP22864A.
[17] Matsui M, Fukushima M, Kubota Y, Funabiki K, Shiro M. Solid-state fluorescence of squarylium dyes. Tetrahedron 2012;68:1931–5https://doi.org/10.1016/j.tet.2011.12.067.
[18] Shafeekh KM, Das S, Sissa C, Painelli A. Asymmetric squaraine dyes: Spectroscopic and theoretical investigation. J Phys Chem 2013;117:8536–46https://doi.org/10.1021/jp401099g.
[19] Gude C, Rettig W. Radiative and nonradiative excited state relaxation channels in squaric acid derivatives bearing differently sized donor substituents: A comparison of experiment and theory. J Phys Chem 2000;104:8050–7https://doi.org/10.1021/jp000139w.
[20] Atwood JL, Gokel GW, Barbour L. Comprehensive supramolecular chemistry II. second ed. Elsevier; 2017.
[21] Jisha VS, Arun KT, Hariharan M, Ramaiah D. Site-selective interactions: Squaraine dye−serum albumin complexes with enhanced fluorescence and triplet yields. J Phys Chem B 2010;114:5912–9https://doi.org/10.1021/jp100369x.
[22] Gonçalves MST. Fluorescent labeling of biomolecules with organic probes. Chem Rev 2009;109:190–212https://doi.org/10.1021/cr0783840.
[23] Karpenko IA, Klymchenko AS, Gioria S, Kreder R, Shulov I, Villa P, Mély Y, Hibert M, Bonnet D. Squaraine as a bright, stable and environment-sensitive far-red label for receptor-specific cellular imaging. Chem Commun 2015;51:2960–3https://doi.org/10.1039/C4CC09113B.
[24] Patsenker L, Tatarets A, Kolosova O, Obukhova O, Povrozin Y, Fedyunyayeva I,

Yermolenko I, Terpetschnig E. Fluorescent probes and labels for biomedical applications. Ann NY Acad Sci 2008;1130:179–87. https://doi.org/10.1196/annals.1430.035.
[25] Hopf H, Sherburn MS. Cross conjugation: Modern dendralene, radialene and fulvene chemistry. Weinheim: Wiley; 2016.
[26] Xia G, Wang H. Squaraine dyes: The hierarchical synthesis and its application in optical detection. J Photochem Photobiol C Photochem Rev 2017;31:84–113https://doi.org/10.1016/j.jphotochemrev.2017.03.001.
[27] Saikiran M, Pandey SS, Hayase Sh, Kato T. Photophysical characterization and BSA interaction of direct ring carboxy functionalized symmetrical squaraine dyes. J Phys: Conf Ser 2017;924. 012006 https://doi.org/10.1088/1742-6596/924/1/012006.
[28] Andrews JH, Khaydarov JDV, Singer KD, Hull DL, Chuang KC. Characterization of excited states of centrosymmetric and noncentrosymmetric squaraines by third-harmonic spectral dispersion. J Opt Soc Am B 1995;12:2360–71https://doi.org/10.1364/JOSAB.12.002360.
[29] Andrews JH, Singer KD, Dirk CW, Hull DL, Chuang KC. Contribution of Two-Photon States to the Third-Order Optical Nonlinearity in Squaraine Compounds. Proc SPIE 1998;3473:68–78https://doi.org/10.1117/12.328177.
[30] Dirk CW, Herndon WC, Cervantes-Lee F, Selnau H, Martinez S, Kalamegham P, Tan A, Campos G, Velez M, Zyss J, Ledoux I, Cheng L-T. Squarylium dyes: Structural factors pertaining to the negative third-order nonlinear optical response. J Am Chem Soc 1995;117:2214–25https://doi.org/10.1021/ja00113a011.
[31] Smith G, Lynch DE. 2-[(3,3-Dimethylindolin-2-ylidene)methyl]-4-[(3,3-dimethyl-3H-indol-1-ium-2-yl)methylidene]-3-oxocyclobut-1-en-1-olate chloroform disolvate. Acta Crystallogr 2013;E69:o786–7https://doi.org/10.1107/S1600536813010386.
[32] Borrelli R, Ellena S, Barolo C. Theoretical and experimental determination of the absorption and emission spectra of a prototypical indolenine-based squaraine dye. Phys Chem Chem Phys 2014;16:2390–8https://doi.org/10.1039/C3CP54298J.
[33] Miltsov S, Encinas C, Alonso J. New cyanine dyes: Norindosquarocyanines. Tetrahedron Lett 1999;40:4067–8https://doi.org/10.1016/S0040-4039(99)00650-4.
[34] Tatarets AL, Fedyunyaeva IA, Terpetschnig E, Patsenker LD. Synthesis of novel squaraine dyes and their intermediates. Dyes Pigments 2005;64:125–34https://doi.org/10.1016/j.dyepig.2004.05.003.
[35] Sheldrick GM. A short history of SHELX. Acta Crystallogr A 2008;A64:112–22https://doi.org/10.1107/S0108767307043930.
[36] Becke AD. Density-functional thermochemistry. III. The role of exact exchange. J Chem Phys 1993;98:5648–52https://doi.org/10.1063/1.464913.
[37] McLean AD, Chandler GS. Contracted Gaussian basis sets for molecular calculations. I. Second row atoms, $Z = 11–18$. J Chem Phys 1980;72:5639–48https://doi.org/10.1063/1.438980.
[38] Gaussian 09, Revision B.01. Wallingford CT: Gaussian, Inc.; 2010.
[39] Glendening ED, Badenhoop JK, Reed AE, Carpenter JE, Bohmann JA, Morales CM, Landis CR, Weinhold F. NBO 6.0. Theoretical Chemistry Institute. Madison, WI: University of Wisconsin; 2013http://nbo6.chem.wisc.edu/.
[40] Patsenker LD, Tatarets AL, Terpetschnig EA. Long-wavelength probes and labels based on cyanines and squaraines. In: Demchenko A, editor. Advanced fluorescence reporters in chemistry and biology I. Springer Series on Fluorescence (Methods and Applications). vol. 8. Berlin, Heidelberg: Springer; 2010. p. 65–104https://doi.org/10.1007/978-3-642-04702-2_3.
[41] Yagi Sh, Nakazumi H. Syntheses and application of squarylium dyes. In: Kim S-H, editor. Functional Dyes. Elsevier; 2006. p. 215–55https://doi.org/10.1016/B978-044452176-7/50007-3.
[42] Tatarets AL, Fedyunyayeva IA, Dyubko TS, YeA Povrozin, Doroshenko AO, Terpetschnig EA, Patsenker LD. Synthesis of water-soluble, ring-substituted squaraine dyes and their evaluation as fluorescent probes and labels. Anal Chim Acta 2006;570:214–23https://doi.org/10.1016/j.aca.2006.04.019.
[43] Kobayashi Y, Goto M, Kurahashi M. The crystal structure of a squarylium dye, 2,4-bis(1,3,3-trimethyl-2-indolinylidenemethyl)cyclobutenediylium-1,3-diolate. Bull Chem Soc Jpn 1986;59:311–2https://doi.org/10.1246/bcsj.59.311.
[44] Burgi H-B, Dunitz JD. Structure correlation vol. 2. Weinheim: VCH; 1994.
[45] Zefirov YuV. Shortened intermolecular contacts and specific interactions in molecular crystals. Kristallographiya (in Russian) 1997;42:936–58.
[46] Markova LI, Terpetschnig EA, Patsenker LD. Comparison of a series of hydrophilic squaraine and cyanine dyes for use as biological labels. Dyes Pigments 2013;99:561–70https://doi.org/10.1016/j.dyepig.2013.06.022.
[47] Parker CA. Photoluminescence of solutions. Amsterdam: Elsevier; 1968.
[48] Collot M, Kreder R, Tatarets AL, Patsenker LD, Mely Y, Klymchenko AS. Bright fluorogenic squaraines with tuned cell entry for selective imaging of plasma membrane *vs.* endoplasmic reticulum. Chem Commun 2015;51:17136–9https://doi.org/10.1039/C5CC06094J.
[49] Terpetschnig E, Szmacinski H, Lakowicz JR. An investigation of squaraines as a new class of fluorophores with long-wavelength excitation and emission. J Fluoresc 1993;3:153–5https://doi.org/10.1007/BF00862734.
[50] Berezin MY, Lee H, Akers W, Achilefu S. Near infrared dyes as lifetime solvatochromic probes for micropolarity measurements of biological systems. Biophys J 2007;93:2892–9http://doi.org/10.1529/biophysj.107.111609.
[51] Patonay G, Salon J, Sowell J, Strekowski L. Noncovalent labeling of biomolecules with red and near-infrared dyes. Molecules 2004;9:40–9https://doi.org/10.3390/90300040.